Second Virial Coefficient of Oligo- and Polystyrenes. Effects of Chain Stiffness on the Interpenetration Function

Hiromi Yamakawa,* Fumiaki Abe, and Yoshiyuki Einaga

Department of Polymer Chemistry, Kyoto University, Kyoto 606-01, Japan

Received November 30, 1992

ABSTRACT: The effect of chain stiffness on the interpenetration function Ψ appearing in the second virial coefficient A_2 is in some detail reexamined theoretically on the basis of the helical wormlike chain. The theory predicts that the chain stiffness has a significant effect on Ψ through those on the intra- and intermolecular excluded-volume interactions even for such large molecular weight M that the ratio of the unperturbed mean-square radius of gyration to M is independent of M. Experimentally, Ψ was determined for atactic polystyrene (a-PS) in toluene at 15.0 °C, in *n*-butyl chloride at 15.0 °C, in 4-*tert*-butyltoluene at 50.0 °C, and in cyclohexane at several temperatures ranging from 40.0 to 55.0 °C in the range of weight-average molecular weight M_w from 5.38×10^3 to 3.84×10^6. These solvents and temperatures were chosen so that the value of the intrinsic viscosity $[\eta]$ for the unperturbed a-PS chain under a given solvent condition might coincide with that of $[\eta]_\Theta$ in cyclohexane at 34.5 °C (Θ). The experimental results are found to be consistent, although only semiquantitatively, with all aspects of the theoretical prediction, revealing that Ψ as a function of the cubed radius expansion factor α_S^3 depends separately also on M_w and on the solvent condition (excluded-volume strength B). Thus the theoretical and experimental findings indicate that the two-parameter theory breaks down completely except for extremely large M and that even a *quasi*-two-parameter scheme is not valid for Ψ, in contrast to the cases of α_S and the viscosity-radius expansion factor α_η.

I. Introduction

In the preceding two papers[1,2] of this series, we have started an experimental reinvestigation of the excluded-volume effects in dilute polymer solutions beyond the framework of the two-parameter theory,[3] determining correctly the radius and viscosity-radius expansion factors α_S and α_η for atactic polystyrene (a-PS) and polyisobutylene over a wide range of molecular weight M. We have explicity demonstrated that the effects of chain stiffness on α_S and α_η remain rather large for such large M that the ratio of the unperturbed mean-square radius of gyration $\langle S^2\rangle_0$ to M already reaches its coil limiting value independent of M. Fortunately, however, it has been found that both α_S and α_η may be expressed as functions only of the scaled excluded-volume parameter $\tilde{z}$ defined in the Yamakawa–Stockmayer–Shimada (YSS) theory[4,5] that takes account of the effects of excluded volume and chain stiffness. The implication is that a *quasi*-two-parameter scheme may be regarded as valid for these single-chain problems. However, such a situation cannot be expected for the second virial coefficient A_2, i.e., a two-chain problem. The purpose of the present and forthcoming papers is to make a detailed analysis, both experimental and theoretical, of A_2 or the interpenetration function Ψ appearing in it.

Now the recent theoretical reanalysis of A_2 by Yamakawa[6] gives attention to both effects of chain stiffness and chain ends in order to explain experimental findings inconsistent with the two-parameter theory prediction. In particular, he has emphasized that the chain stiffness has a significant effect on Ψ even for large M mentioned above, so that Ψ is not a universal function of α_S but its change with α_S depends separately also on M and on the excluded-volume strength (or solvent power) B. The decrease in Ψ with increasing M in good solvents (at fixed B), which has been observed experimentally,[7-10] had already been given an explanation, although for the region of low M, by Huber and Stockmayer,[9] who had examined the effect of chain stiffness by the use of the Yamakawa–Stockmayer (YS) theory.[4] On the other hand, the effect of chain ends becomes appreciable for relatively small M, and it may possibly explain the observed nonvanishing[9,11,12] of A_2 for small M at the Θ temperature (i.e., the temperature at which it vanishes for large M). Thus, in the present paper, we examine in detail the behavior of Ψ as a function of α_S^3 not only at fixed B but also at fixed M for a-PS in good, medium, and poor (Θ) solvents except for such low M that the effect of chain ends cannot be neglected.

Experimentally, the temperature at which A_2 and the mean-square radius of gyration $\langle S^2\rangle$ are to be measured in a given non-Θ solvent must be chosen so that the unperturbed dimension $\langle S^2\rangle_0$ of the a-PS chain in that solvent may coincide with that in the Θ state, as claimed in the previous papers.[1,2] Thus we have measured the intrinsic viscosity $[\eta]$ of oligostyrene samples before measurements of A_2 and $\langle S^2\rangle$ to confirm that their values of $[\eta]$ under the non-Θ solvent conditions chosen in this work are identical with the unperturbed values $[\eta]_\Theta$ in cyclohexane at 34.5 °C (Θ) taken as a reference standard. Recall that according to the previous finding,[1] we may use toluene at 15.0 °C as a suitable good solvent for a-PS.

Before proceeding to the Experimental Section (section III), in the next section we expand somewhat the previous theoretical analysis and discussion of Ψ in order to show explicitly the individual contributions of Ψ of the effects of chain stiffness on $\langle S^2\rangle_0$ and the intra- and intermolecular excluded-volume interactions. This is also useful for a discussion of the present experimental results, since we do not attempt to make a quantitative comparison between theory and experiment. In anticipation of the results, we note that this is due to the fact that it is difficult to obtain the complete quantitative agreement between theory and experiment even if the parameter B is assigned a proper value different from that determined from α_S.

II. Theoretical Section

Corresponding to the YSS theory of α_S, Yamakawa[6] has extended the YS theory of A_2 for the wormlike chain to the helical wormlike (HW) chain,[13,14] with a modification of the functional form of Ψ. Thus, for convenience, we begin by reproducing some of the derived equations that are required for the present discussion. The HW chain may be described essentially in terms of the three model parameters: the constant curvature κ_0 and torsion τ_0 of its

0024-9297/93/2226-1898$04.00/0

characteristic helix taken at the minimum zero of its elastic energy and the static stiffness parameter λ^{-1}. All lengths are measured, as usual, in units of λ^{-1} unless specified otherwise.

Now the interpenetration function Ψ in general is defined in the equation

$$A_2 = 4\pi^{3/2}N_A(\langle S^2\rangle^{3/2}/M^2)\Psi \quad (1)$$

with N_A the Avogadro number. For the chain of total contour length L, it is convenient to factor Ψ as

$$\Psi = C_0\Psi^* \quad (2)$$

with

$$C_0 = \left[\frac{(\langle S^2\rangle_0/L)_\infty}{(\langle S^2\rangle_0/L)}\right]^{3/2} = \left[\frac{(\langle S^2\rangle_0/M)_\infty}{(\langle S^2\rangle_0/M)}\right]^{3/2} \quad (3)$$

where $\langle S^2\rangle_0$ is given by eq 1 of ref 6 as a function $f(L;\kappa_0,\tau_0)$ of L and also κ_0 and τ_0, and the subscript ∞ indicates the limit of L (or M) $\to \infty$. Then eq 2 is the defining equation for Ψ^*.

The function Ψ^* is given by

$$\Psi^* = \tilde{z}h \quad (4)$$

where the so-called h function is equal to A_2 divided by the single-contact term[3] and

$$\tilde{z} = z/\alpha_S^3 \quad (5)$$

with

$$z = (3/2\pi)^{3/2}BL^{1/2} \quad (6)$$

The explicit definition[6] of the excluded-volume strength B, which is proportional to the binary cluster integral β between beads, is unnecessary as far as it is treated as a parameter.

It is assumed that α_S and h are functions only of the parameters $\tilde{z}$ and $\hat{z}$, respectively, which are defined by

$$\tilde{z} = (3/4)K(L)z \quad (7)$$

$$\hat{z} = [Q(L)/2.865]\tilde{z} \quad (8)$$

where the coefficients K and Q as functions only of L are given by eqs 9 and 19 of ref 6, respectively. As for the functional form of α_S, we assume the Domb–Barrett equation[15] with $\tilde{z}$ in place of z, i.e.,

$$\alpha_S^2 = [1 + 10\tilde{z} + (70\pi/9 + 10/3)\tilde{z}^2 + 8\pi^{3/2}\tilde{z}^3]^{2/15} \times [0.933 + 0.067\exp(-0.85\tilde{z} - 1.39\tilde{z}^2)] \quad (9)$$

On the other hand, the functional form of h derived previously[6] from the Barrett function[16] $h(z)$ reads

$$h(\hat{z}) = (1 + 7.74\hat{z} + 52.3\hat{z}^{27/10})^{-10/27} \quad (10)$$

We note that the two-parameter theory (or coil limiting) values of the function h calculated from eq 10 with eq 9 with $\hat{z} = \tilde{z}$ and $\tilde{z} = z$ are very close to those of his original function $h(z)$.

As shown previously in Figure 1 of ref 6, we have examined numerically the behavior of Ψ, taking as an example the case of a-PS, for which $\kappa_0 = 3.0$ and $\tau_0 = 6.0$.[17] In Figure 1 are shown in more detail values of Ψ calculated as a function of α_S^3 from eq 2 with eqs 3–10. The dotted curve represents the two-parameter theory (coil limiting) values mentioned above. The solid curves represent the values for the case in which L (or M) is changed at fixed B, while the dashed curves represent the values for the case in which B is changed at fixed L (or M). It is seen that the two-parameter theory prediction is obtained as the asymptotic limit of $L \to \infty$ or $B \to 0$. As α_S^3 is increased from unity at fixed finite B, Ψ always first decreases and then approaches, although very gradually, the two-parameter theory limiting value 0.231, exhibiting a minimum for small B but without reaching zero. On the other hand, as α_S^3 is increased from unity at fixed finite L, Ψ increases monotonically from zero to (mathematical) asymptotic values larger than the two-parameter theory limiting value, depending on L. (We note that the limit $B \to \infty$ and hence these asymptotic values cannot be realized physically.)

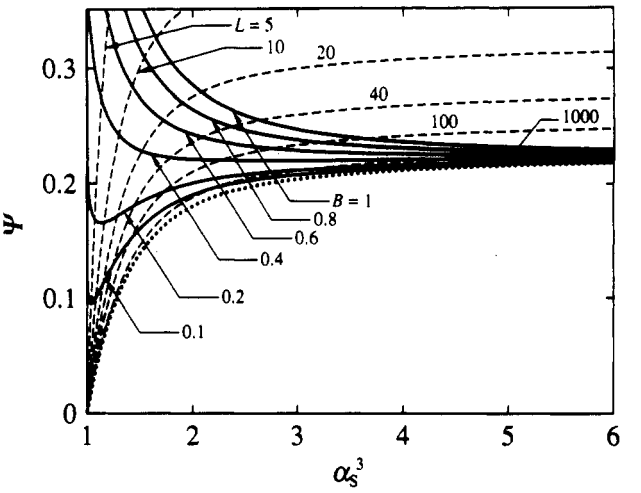

Figure 1. Ψ plotted against α_S^3. The solid and dashed curves represent the values at fixed B and L, respectively, and the dotted curve represents the two-parameter theory values (see the text).

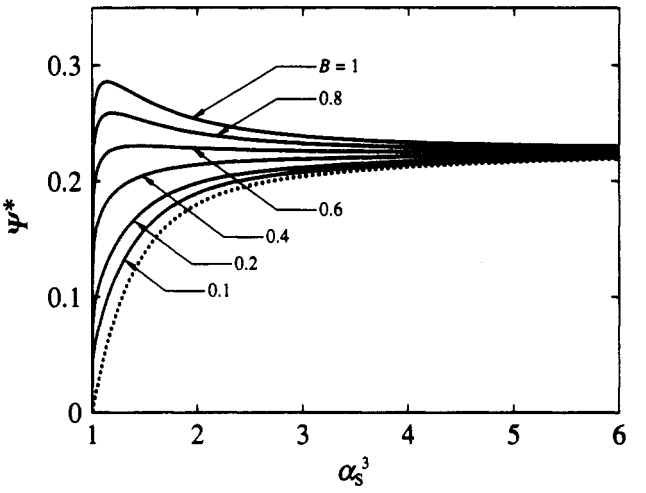

Figure 2. Ψ^* plotted against α_S^3 at fixed B. The dotted curve has the same meaning as that in Figure 1.

Now it is evident that the sharp increase in Ψ with decreasing L (decreasing α_S at fixed B) at small L arises from the prefactor C_0 of Ψ, i.e., the effect of chain stiffness on the unperturbed dimension $\langle S^2\rangle_0$. It is therefore interesting to examine the behavior of the function Ψ^* without C_0. Note that it can also be determined experimentally, as seen from eqs 2 and 3. Clearly, Ψ^* is affected by the chain stiffness only through the effects on the intra- and intermolecular excluded-volume interactions. Figure 2 shows plots of Ψ^* against α_S^3 at fixed B. The dotted curve has the same meaning as that in Figure 1. It is then important to see that without the prefactor, Ψ^* is always appreciably larger than the two-parameter theory prediction and still increases with decreasing L (or α_S) for relatively large B except in the range of α_S close to unity.

Table I
Values of M_w, M_w/M_n, and $\langle S^2\rangle_0^{1/2}$ in Cyclohexane at 34.5 °C (Θ) for Atactic Oligo- and Polystyrenes

sample	$10^{-4}M_w$[a]	M_w/M_n	$\langle S^2\rangle_0^{1/2}$,[b] Å
A5000-3	0.538	1.03	19.0
F1-2	1.01	1.03	27.3
F2	2.05	1.02	39.7
F20	19.1	1.02	
F40	35.9	1.01	167
F80	73.2	1.01	240
F128-2	132	1.05	319
F380	384	1.05	554

[a] The values of M_w had been determined from LS in methyl ethyl ketone at 25.0 °C for A5000-3 and F1-2,[17] in toluene at 15.0 °C for F20,[1] and in cyclohexane at 34.5 °C for the others.[1,11,19] [b] The values of $\langle S^2\rangle_0^{1/2}$ had been determined from SAXS for A5000-3, F1-2, and F2[11] and from LS for the others.[1,19]

This gives a theoretical explanation of the behavior of Ψ that has often been observed experimentally[7,8,10] for flexible polymers in good solvents in the range of M of ordinary interest in the field such that $\langle S^2\rangle_0/M$ is independent of M, so that $C_0 = 1$. In the range of α_S close to unity, Ψ* decreases to zero with decreasing L, exhibiting a maximum for relatively large B, in contrast to Ψ (at fixed B).

In sum, it should again be emphasized that the chain stiffness has significant effects on Ψ as well as on the expansion factors α_S and α_η even for large M mentioned above and that this is due to the slow convergence of the coefficients K and Q in eqs 7 and 8 to the respective coil limiting values $^4/_3$ and 2.865 for $L \to \infty$.

III. Experimental Section

Materials. All the a-PS samples used in this work are the same as those used in the previous studies of the mean-square optical anisotropy $\langle\Gamma^2\rangle$,[17] $[\eta]_0$,[18] $[\eta]$,[2] $\langle S^2\rangle_0$,[11] $\langle S^2\rangle$,[1] the transport factors ρ and Φ for long flexible chains,[19] and the translational diffusion coefficient D,[20] i.e., the fractions separated by preparative gel permeation chromatography (GPC) or fractional precipitation from the standard samples supplied by Tosoh Co., Ltd. They are sufficiently narrow in molecular weight distribution and have a fixed stereochemical composition (the fraction of racemic diads $f_r = 0.59$) independent of molecular weight. The values of the weight-average molecular weight M_w obtained from light scattering (LS) measurements are given in Table I along with those of the ratio of M_w to the number-average molecular weight M_n determined from GPC. It also includes the values of $\langle S^2\rangle_0^{1/2}$ obtained previously from small-angle X-ray scattering (SAXS) and LS measurements in cyclohexane at 34.5 °C (Θ). In addition to the samples listed in Table I, the oligomer samples OS8 (M_w = 904), A2500-a (M_w = 2270), and A2500-b (M_w = 3480)[1,2,18] were also used for viscosity measurements, along with two further additional samples A1000-d and A2500-b′ with viscosity-average molecular weights of 1610 and 2510, respectively. (These values were determined from those of $[\eta]_0$ in cyclohexane at 34.5 °C.)

The solvents toluene, cyclohexane, and *n*-butyl chloride were purified according to standard procedures. The solvent 4-*tert*-butyltoluene was purified by distillation under reduced pressure in a dried nitrogen atmosphere after refluxing over sodium.

Viscosity. Viscosity measurements were carried out for five oligostyrene samples with M_w ranging from 904 to 3480 in order to choose suitable solvents and temperatures at which A_2 and $\langle S^2\rangle$ are to be measured in those solvents, as mentioned in the Introduction. In the preliminary experiments, $[\eta]$ was determined in *n*-butyl chloride and 4-*tert*-butyltoluene at a few temperatures and in cyclohexane at 55.0 °C. For samples A1000-d and A2500-b′, the values of $[\eta]_0$ were also obtained in cyclohexane at 34.5 °C (Θ). We used spiral capillary viscometers of the Ubbelohde type to have long flow times of the test solutions and solvents so that the relative and specific viscosities might be determined with sufficient accuracy. Density corrections were made in the calculation of the relative viscosity from the flow times of the solution and solvent.

The test solutions were prepared gravimetrically and their polymer mass concentrations c (in g/cm^3) were calculated from their weight fractions by using the densities of the respective solutions measured with a pycnometer of the Lipkin–Davison type.

Light Scattering. LS measurements were carried out to obtain A_2 and $\langle S^2\rangle$ (and also M_w) for the a-PS samples in toluene at 15.0 °C, in *n*-butyl chloride at 15.0 °C, in 4-*tert*-butyltoluene at 50.0 °C, and in cyclohexane at several temperatures ranging from 40.0 to 55.0 °C. A Fica 50 light-scattering photometer was used for all the measurements with vertically polarized incident light of wavelength 436 nm. For a calibration of the apparatus, the intensity of light scattered from pure benzene was measured at 25.0 °C at a scattering angle of 90°, where the Rayleigh ratio $R_{vv}(90°)$ of pure benzene was taken as 46.5×10^{-6} cm^{-1}. The depolarization ratio ρ_u of pure benzene at 25.0 °C was determined to be 0.41 ± 0.01. The scattering intensities were measured for at least five solutions of different concentrations for each polymer sample and for the solvent at scattering angles θ ranging from 15 to 150°. The data obtained were analyzed by the Berry square-root plot.[21] (For sample A5000-3 in 4-*tert*-butyltoluene at 50.0 °C and samples A5000-3 and F1-2 in cyclohexane at 50.0 °C, measurements were performed for eight to ten solutions of different concentrations $c < 0.08$ g/cm^3 and the data obtained were analyzed not only by the Berry square-root plot but also by the Bawn plot.[22,23])

The most concentrated solution of each sample in the respective solvent was prepared gravimetrically and made homogeneous by continuous stirring for 1–7 days at ca. 50 °C for the cyclohexane solutions and at room temperature for the others. They were optically purified by filtration through a Teflon membrane of pore size 0.10–0.45 μm. The solutions of lower concentrations were obtained by successive dilution. The polymer mass concentrations c were calculated from the weight fractions by using the densities of the solutions.

The values of the refractive index increment $\partial n/\partial c$ measured for a-PS in *n*-butyl chloride at 15.0 °C and in 4-*tert*-butyltoluene at 50.0 °C at 436 nm by the use of a Shimadzu differential refractometer were 0.206 and 0.120$_6$ cm^3/g, respectively. The values of $\partial n/\partial c$ reported by Miyaki[24] were used for a-PS in cyclohexane at various temperatures.

Small-Angle X-ray Scattering. SAXS measurements were carried out to obtain $\langle S^2\rangle$ for samples F2 and A5000-3 in 4-*tert*-butyltoluene at 50.0 °C and for F2, F1-2, and A5000-3 in cyclohexane at 50.0 °C by using an Anton Paar Kratky U-slit camera with an incident X-ray of wavelength 1.54 Å (Cu Kα line). The apparatus system and the method of data acquisition and analysis are the same as those described in the previous paper.[11]

The measurements were performed for five or six solutions of different concentrations for each polymer sample and for the solvent at scattering angles ranging from 1×10^{-3} rad to a value at which the scattering intensity was negligibly small. Corrections for the stability of the X-ray source and the detector electronics were made by measuring the intensity scattered from Lupolene (a platelet of polyethylene) used as a working standard before and after each measurement of a given sample solution and the solvent. The effect of absorption of X-ray by a given solution or solvent was also corrected by measuring the intensity scattered from Lupolene with insertion of the solution or solvent between the X-ray source and Lupolene. The degree of absorption increased linearly with increasing solute concentration.

The excess reduced scattering intensities were obtained from the observed (smeared) excess reduced intensities by the modified Glatter desmearing method, which consists of expressing the true scattering function in terms of cubic B-spline functions, as described previously.[11] All the data were processed by the use of a Fujitsu M-1800/30 digital computer in this university. Then the desmeared excess reduced intensities were analyzed by the Berry square-root plot as in the case of LS measurements to determine the apparent mean-square radius of gyration $\langle S^2\rangle_z$.[11] Then $\langle S^2\rangle$ (of the chain contour) was obtained from $\langle S^2\rangle_z$ as

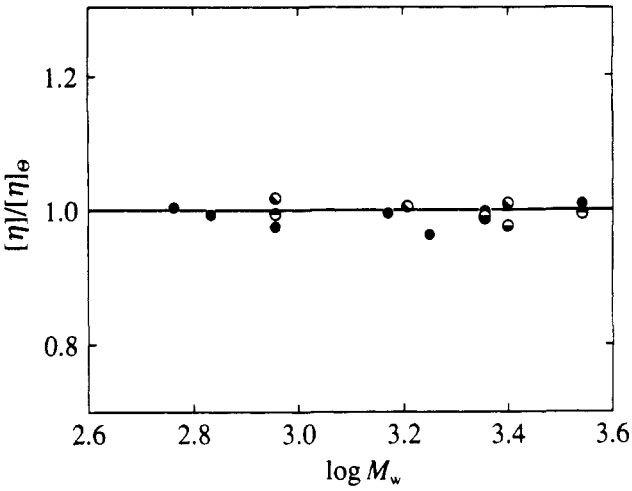

Figure 3. Ratio of $[\eta]$ to $[\eta]_\Theta$ (in cyclohexane at 34.5 °C) plotted against log M_w for oligostyrene: (●) in toluene at 15.0 °C;[1] (◒) in *n*-butyl chloride at 15.0 °C; (◔) in 4-*tert*-butyltoluene at 50.0 °C; (◓) in cyclohexane at 55.0 °C.

before by the use of the equation

$$\langle S^2\rangle_s = \langle S^2\rangle + S_c^2 \qquad (11)$$

which was derived for a continuous chain having a uniform circular cross section with S_c being the radius of gyration of the cross section.[11] In this work, we make the above correction by adopting the value 11 Å^2 for S_c^2 estimated from the data for the partial specific volume of a-PS in cyclohexane at 34.5 °C, as done previously.[1,11]

The solutions of each sample were prepared in the same manner as in the case of LS measurements.

IV. Experimental Results

Intrinsic Viscosities of Atactic Oligostyrenes in Various Solvents. Figure 3 shows plots of the ratio of $[\eta]$ to $[\eta]_\Theta$ against log M_w for the oligostyrene samples in toluene at 15.0 °C (filled circles), in *n*-butyl chloride at 15.0 °C (bottom-half-filled circles), in 4-*tert*-butyltoluene at 50.0 °C (bottom-left-half-filled circles), and in cyclohexane at 55.0 °C (top-half-filled circles) in the range of M_w from 578 to 3480, for which the excluded-volume effect on $[\eta]$ may be neglected. Here, the results for the toluene solution have been reproduced from ref 1 with the values of $[\eta]_\Theta$ determined previously[18] for the same samples in cyclohexane at 34.5 °C (Θ), except for samples A1000-d and A2500-b′, for which the values of $[\eta]_\Theta$ were obtained in this work. It is seen that all the values of the ratio $[\eta]/[\eta]_\Theta$ obtained under the solvent conditions examined are close to unity within experimental errors. The results in cyclohexane at 55.0 °C indicate that the temperature dependence of the *unperturbed* $[\eta]$ for a-PS in cyclohexane is negligibly small in the temperature range from 34.5 to 55.0 °C. Thus we may conclude that the molecular dimensions of these oligomers are the same under the solvent conditions examined, provided that the hydrodynamic diameters of the a-PS chain in these solvents are the same (with the same Flory–Fox factor Φ). (We note that the conclusion has already been confirmed for a-PS in toluene at 15.0 °C by a direct determination of $\langle S^2\rangle$ from SAXS measurements.[1]) According to these findings, we have decided to use these solvents at the temperatures indicated above as good, medium, and poor solvents for a-PS suitable for the present purpose.

Mean-Square Radius of Gyration. The values of $\langle S^2\rangle^{1/2}$ obtained from LS and SAXS measurements are given in the fourth columns of Tables II and III, along with those of M_w and A_2 determined from LS measurements. Table II also includes the results for $\langle S^2\rangle^{1/2}$, M_w, and A_2 obtained previously[1] for the same a-PS samples in toluene at 15.0 °C. Figure 4 shows double-logarithmic plots of $[(\langle S^2\rangle/M_w)/(\langle S^2\rangle_0/M_w)_\infty]$ against M_w for the present results (half-filled and unfilled circles) for a-PS under the various solvent conditions along with those obtained previously in toluene at 15.0 °C (filled circles)[1] and in cyclohexane at 34.5 °C (Θ) (triangles).[1,11,19] Here, $(\langle S^2\rangle_0/M_w)_\infty$ has been taken as 0.0782 Å^2 from the average value of the LS data for the five highest-molecular-weight samples in cyclohexane at Θ. The solid curves connect the data points smoothly.

It is seen that for large M_w, the data points for each fixed solvent condition except for those in cyclohexane at Θ follow a curve convex downward and deviate upward progressively from the latter with increasing M_w because of the excluded-volume effect. At constant M_w, the ratio $[(\langle S^2\rangle/M_w)/(\langle S^2\rangle_0/M_w)_\infty]$ takes the largest value for the toluene solution and decreases in the order of the *n*-butyl chloride, 4-*tert*-butyltoluene, and cyclohexane solutions. The results indicate that toluene and cyclohexane are good and poor solvents, respectively, for a-PS, and both *n*-butyl chloride and 4-*tert*-butyltoluene are medium solvents.

We note that all the a-PS samples used for the present study of A_2 and Ψ have values of M_w such that the ratio

Table II
Results of LS Measurements on Atactic Oligo- and Polystyrenes in Good and Medium Solvents

sample	solvent (temp, °C)	$10^{-4}M_w$	$\langle S^2\rangle^{1/2}$, Å	10^4A_2, cm^3 mol g^{-2}
A5000-3	toluene (15.0)	0.537	20.4[a]	12.2
F2		2.00	43.2[a]	8.80
F20[b]		19.1	162	4.36
F40[b]		35.7	238	3.72
F80[b]		72.3	363	3.12
F128-2[b]		129	520	2.81
F380[b]		394	984	2.07
F40	*n*-butyl chloride (15.0)	36.0	208	2.48
F80		73.9	316	2.00
F128-2		127	448	1.81
F380		392	860	1.35
A5000-3	4-*tert*-butyltoluene (50.0)	0.537	19.5[a]	5.12
F2		2.02	41.7[a]	4.18
F40		36.4	204	2.03
F80		74.3	313	1.74
F128-2		128	438	1.55
F380		395	826	1.17

[a] From SAXS measurements. The data in toluene have been reproduced from ref 1. [b] The results have been reproduced from ref 1 except for A_2, the values of which were not reported there, although already determined.

Table III
Results of LS Measurements on Atactic Oligo- and Polystyrenes in Cyclohexane at Various Temperatures

sample	temp, °C	$10^{-4}M_w$	$\langle S^2\rangle^{1/2}$, Å	10^4A_2, cm^3 mol g^{-2}
F40	40.0	37.0	169	0.320
F80		74.4	253	0.304
F128-2		127	342	0.321
F40	45.0	37.0	172	0.526
F80		74.3	258	0.537
F128-2		128	358	0.509
A5000-3	50.0	0.548	19.2[a]	2.50
F1-2		1.03	27.9[a]	1.62
F2		2.05	40.7[a]	1.20
F40		37.0	175	0.764
F80		74.6	269	0.738
F128-2		128	369	0.674
F40	55.0	37.0	177	0.887
F80		74.6	273	0.854
F128-2		128	378	0.797

[a] From SAXS measurements.

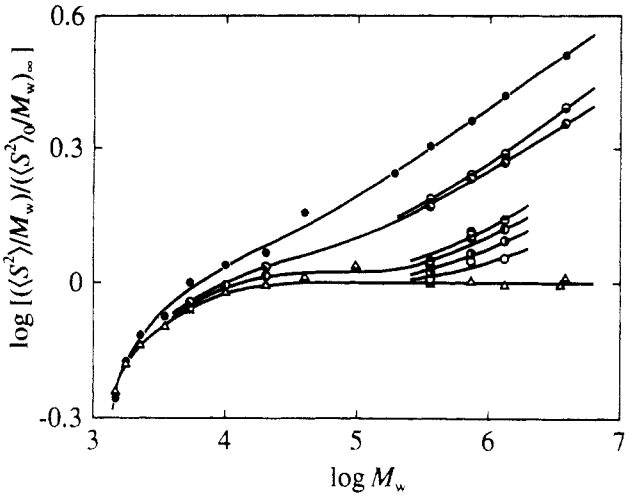

Figure 4. Double-logarithmic plots of $[(\langle S^2\rangle/M_w)/(\langle S^2\rangle_0/M_w)_\infty]$ against M_w for the a-PS samples (with $f_r = 0.59$): (●) in toluene at 15.0 °C;[1] (◒) in *n*-butyl chloride at 15.0 °C; (◔) in 4-*tert*-butyltoluene at 50.0 °C; (◓) in cyclohexane at 55.0 °C; (◐) in cyclohexane at 50.0 °C; (◑) in cyclohexane at 45.0 °C; (○) in cyclohexane at 40.0 °C; (△) in cyclohexane at 34.5 °C (Θ) (for which, $\langle S^2\rangle/M_w$ means $\langle S^2\rangle_0/M_w$).[1,11,19]

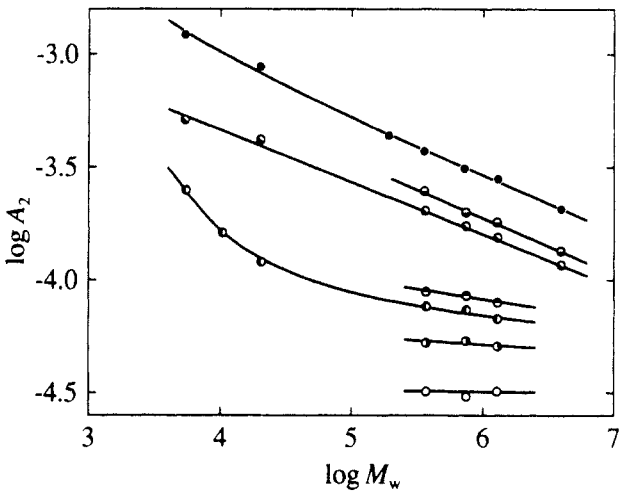

Figure 5. Double-logarithmic plots of A_2 against M_w. The symbols have the same meaning as those in Figure 4.

$\langle S^2\rangle_0/M_w$ almost reaches its coil limiting value except for the lowest-molecular-weight sample A5000-3, for which the above ratio is ca. 13% smaller than the limiting value.

Second Virial Coefficient. The values of A_2 obtained from LS measurements are listed in the fifth columns of Tables II and III and are double-logarithmically plotted against M_w in Figure 5. The variation of A_2 with solvent condition at fixed M_w is in the same order as that of $[(\langle S^2\rangle/M_w)/(\langle S^2\rangle_0/M_w)_\infty]$ shown in Figure 4, indicating the consistency of the experimental results for A_2 and $\langle S^2\rangle$. It is seen that A_2 increases with decreasing M_w for the toluene solution, following a curve slightly convex downward, and it steeply increases with decreasing M_w for small M_w for the cyclohexane solution at 50.0 °C. The absolute value of the slope of the former curve is ca. 0.25 or larger. These results are clearly in conflict with the two-parameter theory prediction, as already discussed by Fujita;[25] the two-parameter theory never predicts such a curve convex downward but a curve convex upward with the maximum absolute slope of 0.2. This observed dependence of A_2 on M_w is equivalent to the observed behavior of Ψ inconsistent with the two-parameter theory prediction, as mentioned in the Introduction.

Table IV
Values of Ψ and α_S^3 for Atactic Oligo- and Polystyrenes in Good and Medium Solvents

sample	solvent (temp, °C)	Ψ	α_S^3
A5000-3	toluene (15.0)	0.310	1.23
F2		0.325	1.29
F20		0.280	(2.32)[a]
F40		0.264	2.88
F80		0.254	3.45
F128-2		0.249	4.31
F380		0.252	5.60
F40	*n*-butyl chloride (15.0)	0.265	1.93
F80		0.258	2.28
F128-2		0.241	2.77
F380		0.244	3.74
A5000-3	4-*tert*-butyltoluene (50.0)	0.148	1.08
F2		0.175	1.16
F40		0.236	1.83
F80		0.236	2.20
F128-2		0.225	2.58
F380		0.240	3.32

[a] The value of α_S^3 has been calculated with the value 0.0782 Å^2 of $(\langle S^2\rangle_0/M_w)_\infty$.[1,19]

Table V
Values of Ψ and α_S^3 for Atactic Oligo- and Polystyrenes in Cyclohexane at Various Temperatures

sample	temp, °C	Ψ	α_S^3
F40	40.0	0.068	1.04
F80		0.078	1.16
F128-2		0.097	1.23
F40	45.0	0.106	1.09
F80		0.128	1.24
F128-2		0.135	1.41
A5000-3	50.0	0.077	1.03
F1-2		0.058	1.07
F2		0.056	1.08
F40		0.147	1.14
F80		0.157	1.40
F128-2		0.164	1.54
F40	55.0	0.162	1.20
F80		0.174	1.47
F128-2		0.180	1.66

V. Discussion

We are now in a position to discuss the observed behavior of Ψ in comparison with the theoretical prediction given in section II. In Tables IV and V are summarized its values calculated from eq 1 with the experimental values of A_2, $\langle S^2\rangle^{1/2}$, and M_w given in Tables II and III, along with the values of α_S^3 calculated from the equation $\alpha_S^2 = \langle S^2\rangle/\langle S^2\rangle_0$ with the values of $\langle S^2\rangle^{1/2}$ in Tables II and III and those of $\langle S^2\rangle_0^{1/2}$ in Table I. All the data for Ψ are plotted against α_S^3 in Figure 6. Here, various types of circles indicate different solvent conditions (different excluded-volume strengths B), and various directions of pips attached to them indicate different molecular weights M_w. This figure also includes the literature data (circles without pip) by Miyaki[24] for the a-PS sample with a very high molecular weight, i.e., $M_w = 3.19 \times 10^7$, in cyclohexane. The solid curves connect smoothly the data points for different M_w at fixed B (at fixed solvent condition), while the dashed curves connect smoothly those for different B at fixed M_w. The dotted curve represents the two-parameter theory (coil limiting) values calculated from eq 2 with eqs 3–10 with $\hat{z} = \tilde{z}$ and $\tilde{z} = z$, as mentioned in section II.

From a comparison with Figure 1, it is seen that the theory may explain, although only semiquantitatively, the overall features of the experimental results in Figure 6. All the data points are clearly seen to deviate significantly upward from the two-parameter theory prediction, except

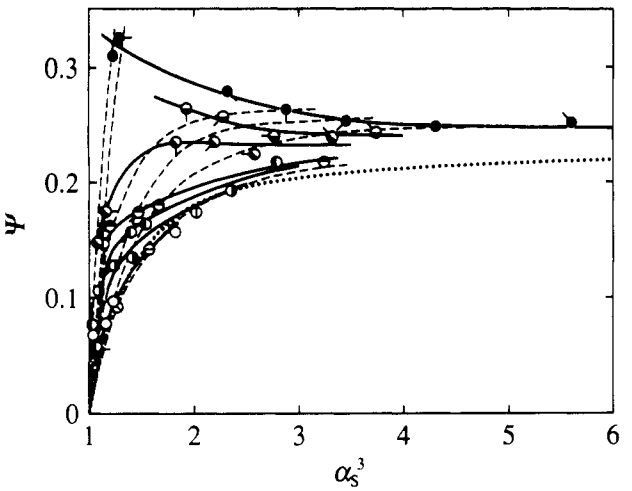

Figure 6. Ψ plotted against α_S^3. Various directions of pips indicate different values of M_w: pip up, 5.38×10^4; successive 45° rotations clockwise correspond to 1.01×10^4, 2.05×10^4, 1.91×10^5, 3.59×10^5, 7.32×10^5, 1.32×10^6, and 3.84×10^6, respectively; no pip, 3.19×10^7 (by Miyaki[24]). Various types of circles indicate different solvent conditions with the same meaning as in Figure 4, except for ⊕ (in cyclohexane at 42.0 °C), ⊖ (in cyclohexane at 38.0 °C), and ⊘ (in cyclohexane at 36.0 °C). The solid and dashed curves smoothly connect the data points at fixed B (solvent condition) and M_w, respectively. The dotted curve represents the two-parameter theory values.

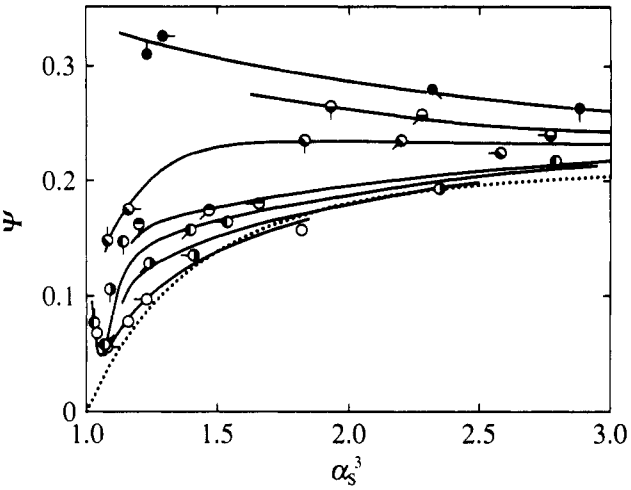

Figure 7. Ψ plotted against α_S^3 at fixed B. The symbols and the dotted curve have the same meaning as those in Figure 6. The solid curves smoothly connect the data points.

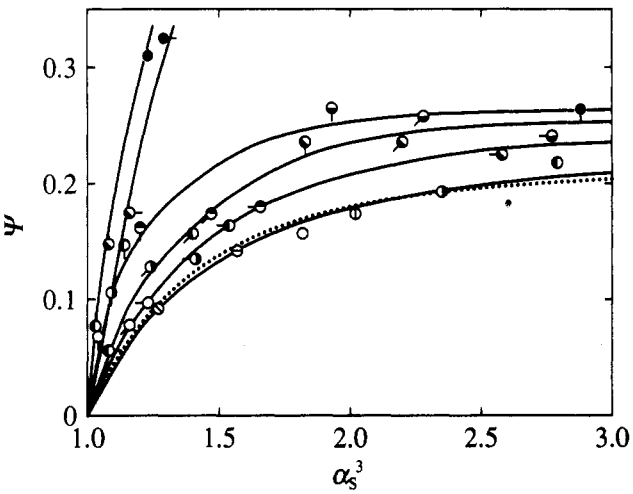

Figure 8. Ψ plotted against α_S^3 at fixed M_w. The symbols and the dotted curve have the same meaning as those in Figure 6. The solid curves smoothly connect the data points.

for the data of Miyaki,[24] which are in fact in agreement with the latter. It is also seen that for the toluene and *n*-butyl chloride solutions Ψ increases with decreasing α_S^3 or decreasing M_w following the respective curves concave upward, as often observed experimentally[7,8,10] and consistent with the present theoretical results shown in the curves with $B \gtrsim 0.4$ in Figure 1. (Note that for the toluene solution the value of B to be assigned is larger than the value 0.26 determined from α_S in the previous paper.[1]) Although for the cyclohexane solutions Ψ decreases with decreasing α_S^3 as the two-parameter theory predicts, it deviates systematically upward from the latter prediction, as shown by the theoretical curves with $B = 0.1$ and 0.2 in Figure 1, to a greater extent as the temperature becomes higher and α_S^3 becomes smaller. For the 4-*tert*-butyltoluene solution, Ψ first increases with increasing α_S^3 and then decreases slightly and gradually. As shown by the dashed curves in Figure 6, as α_S^3 (or B) is increased at fixed M_w, Ψ first increases following the separate curves, depending on M_w, and then it levels off to higher values for smaller M_w (except for the two lowest M_w). It is important to note that the disagreement between the observed dependence of Ψ on α_S^3 and the two-parameter theory prediction occurs in the range of ordinary M_w extensively studied so far.

The plots in the region of small α_S^3 (and small Ψ) are rather complicated in Figure 6. Thus this region is enlarged in Figures 7 and 8 in order to display more clearly the dependence of Ψ on α_S^3 at fixed B and at fixed M_w, respectively. It is seen from Figure 7 that the plot for the cyclohexane solution at 50.0 °C exhibits a sharp minimum of Ψ at $\alpha_S^3 \simeq 1.05$, corresponding to the theoretical results shown in the curves with $B = 0.1$ and 0.2 in Figure 1, although the observed minimum value is much smaller. It is seen from Figure 8 that there is good agreement between Miyaki's data and the two-parameter theory values. This implies that the effect of chain stiffness may be regarded as completely negligible for the a-PS chain with $M_w = 3.19 \times 10^7$. However, the observed Ψ exhibits a more rapid increase with increasing α_S^3 (or B) for smaller M_w, being inconsistent with the two-parameter theory prediction but consistent with the present theoretical results shown in the dashed curves in Figure 1.

As discussed in section II, the chain stiffness has an effect on Ψ through the effects on the unperturbed chain dimension $\langle S^2 \rangle_0$ and the excluded-volume interactions, so that we have factored Ψ into C_0 and Ψ* as in eq 2 to examine the two effects separately. Indeed, the function Ψ* is affected only by the latter, and it is this part that may describe mainly the above experimental results for Ψ, the two functions being very close to each other except for the lowest three samples with $M_w \leq 2.05 \times 10^4$. Thus the results for Ψ* calculated from eq 2 with eq 3 with the experimental values of Ψ and $\langle S^2 \rangle_0 / M_w$ are shown in Figure 9, where the dotted curve again represents the two-parameter theory values. It is seen that the data points for sample A5000-3 (M_w = 5380) move appreciably downward compared to those in Figure 7, giving rise to a maximum of Ψ* for the toluene solution. There is qualitative (or semiquantitative) agreement between the observed curves in Figure 9 and the theoretical curves in Figure 2.

Thus it may be concluded that except for extremely large M_w, Ψ as a function of α_S^3 deviates upward from the two-parameter theory values because of the effect of chain stiffness mainly through those on the excluded-volume interactions, the deviation being rather appreciable even in the range of large α_S^3.

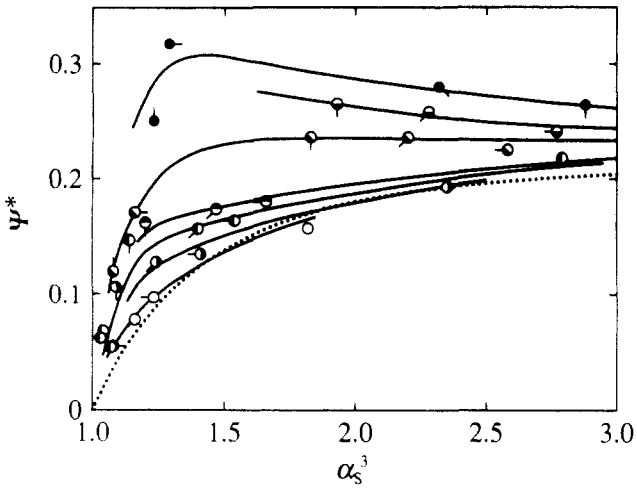

Figure 9. Ψ^* plotted against α_S^3 at fixed B. The symbols and the dotted curve have the same meaning as those in Figure 6. The solid curves smoothly connect the data points.

VI. Conclusion

In this paper, we have expanded the previous theoretical analysis and discussion[6] of Ψ in order to show explicitly the manner in which the chain stiffness has an effect on it. The effect is found to remain rather significant mainly through those on the intra- and intermolecular excluded-volume interactions even for such large M that the ratio $\langle S^2\rangle_0/M$ is independent of M. The experimental results for Ψ for a-PS under various solvent conditions are consistent, although only semiquantitatively, with all salient aspects of the theoretical prediction, revealing that Ψ as a function of α_S^3 depends separately also on the molecular weight M_w and on the solvent condition (excluded-volume strength B). Possible effects of chain ends on Ψ, which cannot be negligible for low M_w, have not been considered in the present work. However, the above conclusion may be unaltered, since most of the present experimental results have been obtained for the samples with such large M_w that they may be neglected. In a forthcoming paper, we make a study of Ψ for such low M_w.

The theoretical and experimental results lead to the conclusion that neither the two-parameter scheme nor even the *quasi*-two-parameter scheme is in general valid for Ψ, in contrast to the cases of α_S and α_η, which may be expressed as functions only of the scaled excluded-volume parameter $\tilde{z}$, as reported in the preceding papers.[1,2] Thus the situation is quite complicated for Ψ (or A_2), differing from the case of the single-chain problems.

Acknowledgment. This research was supported in part by a Grant-in-Aid (0245 3100) from the Ministry of Education, Science, and Culture, Japan.

References and Notes

(1) Abe, F.; Einaga, Y.; Yoshizaki, T.; Yamakawa, H. *Macromolecules*, preceding paper in this issue.
(2) Abe, F.; Einaga, Y.; Yamakawa, H. *Macromolecules*, preceding paper in this issue.
(3) Yamakawa, H. *Modern Theory of Polymer Solutions*; Harper & Row: New York, 1971.
(4) Yamakawa, H.; Stockmayer, W. H. *J. Chem. Phys.* **1972**, *57*, 2843.
(5) Shimada, J.; Yamakawa, H. *J. Chem. Phys.* **1986**, *85*, 591.
(6) Yamakawa, H. *Macromolecules* **1992**, *25*, 1912.
(7) Miyaki, Y.; Einaga, Y.; Fujita, H. *Macromolecules* **1978**, *11*, 1180.
(8) Hirosye, T.; Einaga, Y.; Fujita, H. *Polym. J.* **1979**, *11*, 819.
(9) Huber, K.; Stockmayer, W. H. *Macromolecules* **1987**, *20*, 1400.
(10) Nakamura, Y.; Akasaka, K.; Katayama, K.; Norisuye, T.; Teramoto, A. *Macromolecules* **1992**, *25*, 1134.
(11) Konishi, T.; Yoshizaki, T.; Saito, T.; Einaga, Y.; Yamakawa, H. *Macromolecules* **1990**, *23*, 290.
(12) Tamai, Y.; Konishi, T.; Einaga, Y.; Fujii, M.; Yamakawa, H. *Macromolecules* **1990**, *23*, 4067.
(13) Yamakawa, H. *Annu. Rev. Phys. Chem.* **1984**, *35*, 23.
(14) Yamakawa, H. In *Molecular Conformation and Dynamics of Macromolecules in Condensed Systems*; Nagasawa, M., Ed.; Elsevier: Amsterdam, 1988; p 21.
(15) Domb, C.; Barrett, A. J. *Polymer* **1976**, *17*, 179.
(16) Barrett, A. J. *Macromolecules* **1985**, *18*, 196.
(17) Konishi, T.; Yoshizaki, T.; Shimada, J.; Yamakawa, H. *Macromolecules* **1989**, *22*, 1921.
(18) Einaga, Y.; Koyama, H.; Konishi, T.; Yamakawa, H. *Macromolecules* **1989**, *22*, 3419.
(19) Konishi, T.; Yoshizaki, T.; Yamakawa, H. *Macromolecules* **1991**, *24*, 5614.
(20) Yamada, T.; Yoshizaki, T.; Yamakawa, H. *Macromolecules* **1992**, *25*, 377.
(21) Berry, G. C. *J. Chem. Phys.* **1966**, *44*, 4550.
(22) Bawn, C. E. H.; Freeman, R. F. J.; Kamaliddin, A. R. *Trans. Faraday Soc.* **1950**, *46*, 862.
(23) Norisuye, T.; Fujita, H. *Chemistracts—Macromolecular Chemistry* **1991**, *2*, 293.
(24) Miyaki, Y. Ph.D. Thesis, Osaka University, 1981.
(25) Fujita, H. *Macromolecules* **1988**, *21*, 179.